

# Scalable Tensor Completion with Nonconvex Regularization

Quanming Yao

4Paradigm Inc.  
Beijing, China  
yaoquanming@4paradigm.com

## Abstract

Low-rank tensor completion problem aims to recover a tensor from limited observations, which has many real-world applications. Due to the easy optimization, the convex overlapping nuclear norm has been popularly used for tensor completion. However, it over-penalizes top singular values and lead to biased estimations. In this paper, we propose to use the nonconvex regularizer, which can less penalize large singular values, instead of the convex one for tensor completion. However, as the new regularizer is nonconvex and overlapped with each other, existing algorithms are either too slow or suffer from the huge memory cost. To address these issues, we develop an efficient and scalable algorithm, which is based on the proximal average (PA) algorithm, for real-world problems. Compared with the direct usage of PA algorithm, the proposed algorithm runs orders faster and needs orders less space. We further speed up the proposed algorithm with the acceleration technique, and show the convergence to critical points is still guaranteed. Experimental comparisons of the proposed approach are made with various other tensor completion approaches. Empirical results show that the proposed algorithm is very fast and can produce much better recovery performance.

## 1 Introduction

Tensors, which can be seen as high-order matrices, have been commonly used to describe the multilinear relationships inside the data. In this paper, we focus on 3-order tensors, since they naturally appear in many applications. For example, the color image can be seen as 3-order tensor (Liu et al. 2013); in remote sensing applications, a hyperspectral image with multiple bands can be naturally represented as a 3-order tensor (Signoretto et al. 2011); in Youtube’s social network, users can follow each other and can have the same subscribed channels. By treating these attributes as another dimension, rating prediction becomes a problem on the 3-order tensor (Lei, Wang, and Liu 2009).

However, usually, we can only have a few observations in these tensors. In the social network mentioned above, users can only explore a few other users. Then, in hyperspectral imaging, some bands may be partially or totally missing due to sensor problems (Signoretto et al. 2011). Therefore, tensor completion is very important for real applications (Song et al. 2017).

Low-rank tensor completion is popularly used for filling and predicting these unseen values (Tomioka, Hayashi, and Kashima 2010; Acar et al. 2011). Mathematically, let the observed elements indicating by 1’s in the binary tensor  $\Omega \in \{0, 1\}^{I_1 \times I_2 \times I_3}$  (assume  $I_1 \geq I_2 \geq I_3$ ) with values given by corresponding positions in  $\mathbf{O} \in \mathbb{R}^{I_1 \times I_2 \times I_3}$ , the low-rank tensor completion problem is

$$\min_{\mathbf{X} \in \mathbb{R}^{I_1 \times I_2 \times I_3}} \frac{1}{2} \|P_{\Omega}(\mathbf{X} - \mathbf{O})\|_F^2 + \lambda r(\mathbf{X}), \quad (1)$$

where  $r$  is a regularizer encouraging the tensor to be low-rank, and  $[P_{\Omega}(\mathbf{X})]_{i_1 i_2 i_3} = \mathbf{X}_{i_1 i_2 i_3}$  if  $\Omega_{i_1 i_2 i_3} = 1$  and 0 otherwise.

Recently, due to the success of the nuclear norm for low-rank matrix completion (Candès and Recht 2009), convex relaxation of tensor rank based on the nuclear norm are also introduced for tensor completion (Tomioka, Hayashi, and Kashima 2010; Gandy, Recht, and Yamada 2011). Common examples of  $r$  include the tensor trace norm (Chandrasekaran et al. 2012), overlapped nuclear norm (Tomioka, Hayashi, and Kashima 2010; Gandy, Recht, and Yamada 2011), and latent nuclear norm (Tomioka, Hayashi, and Kashima 2010).

Unlike traditional low-rank tensor completion approaches, which are based on canonical polyadic (CP) or Tucker decompositions (Kolda and Bader 2009), the optimization then becomes a convex problem, which can be solved with the convergence guarantee. Among them, the overlapped nuclear norm is the most popular ones. Compared with the tensor trace norm, it can be computed exactly without the approximation (Cheng et al. 2016). Then, it can encourage tensor to be low-rank on every mode simultaneously, which can better approximate a low-rank tensor than the latent nuclear norm (Tomioka, Hayashi, and Kashima 2010). Besides, the theoretical guarantee has also been provided, which shows the exact recovery is possible (Tomioka et al. 2011; Tomioka and Suzuki 2013; Mu et al. 2014).

However, one potential problem of the nuclear norm is that it equally penalizes all singular values, while the larger singular values can be more informative (Mazumder, Hastie, and Tibshirani 2010). To less penalize large singular values, adaptive nonconvex regularizers, have been introduced for low-rank matrix learning. Examples are, capped- $\ell_1$  norm

(Zhang 2010b), log-sum-penalty (LSP) (Candès, Wakin, and Boyd 2008), truncated nuclear norm (TNN) (Hu et al. 2013), smoothed-capped-absolute-deviation (SCAD) (Fan and Li 2001) and minimax concave penalty (MCP) (Zhang 2010a). They give both better empirical performance (Lu et al. 2016; Yao et al. 2017b; Mazumder, Saldana, and Weng 2018) and statistical guarantee (Gui, Han, and Gu 2016) than the convex nuclear norm. Besides, these regularizers have not been used for tensor completion yet.

Motivating by the problem of over-penalizing top singular values of the convex nuclear norm, we propose to use nonconvex penalties with overlapped nuclear norm as  $r$  in (1). Since the regularizers are nonconvex and overlap with each other, the resulting problem is hard to optimize. We first find that the proximal average (PA) algorithm (Zhong and Kwok 2014) becomes the only applicable algorithm which also has the convergence guarantee.

Unfortunately, due to the needs of folding and unfolding operations of tensor, PA algorithm suffers from the extremely large space requirement and expensive iteration complexity. These greatly limit the usage of the new model in real problems, especially when the data scale is large. To address these issues, we propose an important proposition avoiding such operations in iterations of PA algorithm. Moreover, we adopt the acceleration technique to speed up the convergence of PA algorithm, while still offers the convergence guarantee. This helps to significantly cut down the number of iterations required by PA algorithm. As a result, the proposed algorithm needs orders less memory but runs orders faster than the direct usage of PA algorithm. Finally, we perform experiments on both synthetic and real data sets. Results show the proposed algorithm is very efficient and can produce much better empirical performance than other tensor regularization and decomposition methods.

The rest of the paper is organized as follows. Section 2 gives the background on related works. The proposed algorithm is in Section 3. Experiments are performed in Section 4. Finally, concluding remarks are given in Section 5. All proofs are in Appendix.A.

**Notation** In the sequel, vectors are denoted by lowercase boldface, matrices by uppercase boldface, and tensors by boldface Euler. For a matrix  $\mathbf{A}$  with singular values  $\sigma_i$ 's, its nuclear norm is  $\|\mathbf{A}\|_* = \sum_i \sigma_i$ . We follow the tensor notations in (Kolda and Bader 2009). For a 3-order tensor  $\mathcal{X} \in \mathbb{R}^{I_1 \times I_2 \times I_3}$ , its  $(i_1, i_2, i_3)$ th entry is  $x_{i_1 i_2 i_3}$ . Let  $I_\times = \prod_{i=1}^M I_i$  and  $I_+ = \sum_{i=1}^M I_i$ , and the mode- $d$  matricizations  $\mathcal{X}_{\langle d \rangle}$  of  $\mathcal{X}$  is a  $I_d \times I_{I_\times / I_d}$  matrix with  $(\mathcal{X}_{\langle d \rangle})_{i_d j} = x_{i_1 i_2 i_3}$ , and  $j = 1 + \sum_{l=1, l \neq d}^3 (i_l - 1) \prod_{m=1, m \neq d}^{l-1} I_m$ . Given a matrix  $\mathbf{A}$ , its mode- $d$  tensorization  $\mathbf{A}^{(d)}$  is a tensor  $\mathcal{X}$  with elements  $x_{i_1 i_2 i_3} = a_{i_d j}$ , and  $j$  is as defined before. The inner product of two tensors  $\mathcal{X}$  and  $\mathcal{Y}$  is  $\langle \mathcal{X}, \mathcal{Y} \rangle = \sum_{i_1=1}^{I_1} \sum_{i_2=1}^{I_2} \sum_{i_3=1}^{I_3} x_{i_1 i_2 i_3} y_{i_1 i_2 i_3}$ , and the Frobenius norm of  $\mathcal{X}$  is  $\|\mathcal{X}\|_F = \sqrt{\langle \mathcal{X}, \mathcal{X} \rangle}$ .

## 2 Related Works

Here, we first describe the usage of nonconvex regularization for low-rank matrix learning in Section 2.1. Then,

the convex regularization for low-rank tensor learning is introduced in Section 2.2. Finally, as the proposed method is built on PA algorithm, we discuss its details in Section 2.3.

### 2.1 Nonconvex Low-Rank Matrix Regularization

As mentioned in Section 1, nonconvex regularizers, such as capped- $\ell$  norm, LSP, TNN, SCAD and MCP, have been introduced in low-rank matrix learning. Unlike the convex nuclear norm and factorization methods, these regularizers can less penalize larger singular values, which are more informative. Thus, they have both better empirical performance and theoretical guarantee than the nuclear norm regularization. (Lu et al. 2016; Gui, Han, and Gu 2016; Yao et al. 2017b; Mazumder, Saldana, and Weng 2018). The optimization problem is formulated as

$$\min_{\mathbf{X} \in \mathbb{R}^{I_1 \times I_2}} f(\mathbf{X}) + \lambda \phi(\mathbf{X}), \quad (2)$$

where  $f$  is a smooth loss (assume  $\rho$ -Lipschitz smooth),

$$\phi(\mathbf{X}) = \sum_{i=1}^{I_2} \kappa(\sigma_i(\mathbf{X})) \quad (3)$$

is the nonconvex regularizer, and  $\kappa$  is the nonconvex penalty (Assumption 1). Popular examples of  $\phi$  are in Table 1.

**Assumption 1.**  $\kappa(\alpha)$  is a concave, nondecreasing and  $L$ -Lipschitz continuous function on  $\alpha \geq 0$  with  $\kappa(0) = 0$ .

Table 1: Examples of nonconvex penalties  $\kappa(\sigma_i(\mathbf{X}))$  where  $\theta$  is a constant. For capped- $\ell_1$ , LSP and MCP,  $\theta > 0$ ; for SCAD,  $\theta > 2$ ; and for TNN,  $\theta$  is a positive integer.

	$\kappa(\sigma_i(\mathbf{X}))$
capped- $\ell_1$ (Zhang 2010b)	$\min(\sigma_i(\mathbf{X}), \theta)$
LSP (Candès, Wakin, and Boyd 2008)	$\log(\frac{1}{\theta} \sigma_i(\mathbf{X}) + 1)$
TNN (Hu et al. 2013)	$\begin{cases} \sigma_i(\mathbf{X}) & \text{if } i > \theta \\ 0 & \text{otherwise} \end{cases}$
SCAD (Fan and Li 2001)	$\begin{cases} \sigma_i(\mathbf{X}) & \text{if } \sigma_i(\mathbf{X}) \leq 1 \\ \frac{2\theta\sigma_i(\mathbf{X}) - \sigma_i(\mathbf{X})^2 - 1}{2(\theta-1)} & \text{if } 1 < \sigma_i(\mathbf{X}) \leq \theta \\ \frac{(\theta+1)^2}{2} & \text{otherwise} \end{cases}$
MCP (Zhang 2010a)	$\begin{cases} \sigma_i(\mathbf{X}) - \frac{\alpha^2}{2\theta} & \text{if } \sigma_i(\mathbf{X}) \leq \theta \\ \frac{\theta^2}{2} & \text{otherwise} \end{cases}$

Problem (2) is a nonconvex problem, which is generally hard to optimize. However, proximal gradient (PG) algorithms (Parikh and Boyd 2013) have been recently developed as an efficient optimization approach for solving (2) (Yao et al. 2017b; Lu et al. 2016; Mazumder, Saldana, and Weng 2018). Basically, at iteration  $t$ , it produces

$$\mathbf{X}_{t+1} = \text{prox}_{\frac{\lambda}{\tau} \phi}(\mathbf{Z}_t), \quad (4)$$

where  $\mathbf{Z}_t = \mathbf{X}_t - \frac{1}{\tau} \nabla f(\mathbf{X}_t)$ ,  $\tau > \rho$  is the stepsize, and

$$\text{prox}_{\frac{\lambda}{\tau} \phi}(\mathbf{Z}) \equiv \text{Arg} \min_{\mathbf{X}} \frac{1}{2} \|\mathbf{X} - \mathbf{Z}\|_F^2 + \frac{\lambda}{\tau} \phi(\mathbf{X}), \quad (5)$$

is the proximal operator (Parikh and Boyd 2013). For nonconvex regularizers (Table 1), fortunately, the closed-form solution on proximal step is in Lemma 2.1.

**Lemma 2.1** ((Lu et al. 2016)). *Let SVD of  $\mathbf{Z} \in \mathbb{R}^{I_1 \times I_2}$  be  $\mathbf{U}\Sigma\mathbf{V}^\top$ , then  $\text{prox}_{\lambda\phi}(\mathbf{Z}) = \mathbf{U}\text{Diag}(y_1, \dots, y_{I_2})\mathbf{V}^\top$  where  $y_i = \arg \min_{y \geq 0} (1/2)(y - \sigma_i(\mathbf{Z}))^2 + \lambda\kappa(y)$ .*

PG algorithms guarantee producing a critical point of (2). However, SVD is needed in Lemma 2.1. A cut-off property is observed in (Yao et al. 2017b), which allows inexact SVD by the power method (Halko, Martinsson, and Tropp 2011). Besides, the acceleration is considered in (Yao et al. 2017a) to speed up the slow convergence of PG algorithms on (2).

## 2.2 Low-Rank Tensor Regularization

Nuclear norm has been popularly used for low-rank matrix learning. Recently, it has also been extended to learn low-rank tensors. However, unlike matrix, the rank of the tensor is not uniquely defined (Hillar and Lim 2013). For tensors, several definitions of the norm exist. The most common ones are the overlapped nuclear norm and the latent nuclear norm (Tomioka, Hayashi, and Kashima 2010; Gandy, Recht, and Yamada 2011), which is in Definition 1.

**Definition 1.** *For a  $M$ -order tensor  $\mathbf{X}$ , the overlapped nuclear norm is  $\|\mathbf{X}\|_{\text{overlap}} = \sum_{m=1}^M \lambda_m \|\mathbf{X}_{\langle m \rangle}\|_*$ , and the latent nuclear norm is  $\|\mathbf{X}\|_{\text{scaled}} = \min_{\mathbf{X}_1, \dots, \mathbf{X}_M : \sum_{m=1}^M \mathbf{X}_d = \mathbf{X}} \sum_{m=1}^M \lambda_m \|\mathbf{X}_m\|_*$ .*

Intuitively, overlapped nuclear norm encourages the tensor to be low-rank on each mode; and latent nuclear norm represents a tensor by a mixture of tensors, each of which is low-rank on one mode. Since overlapped nuclear norm directly models the low-rank tensor as a whole, it usually has better empirical performance than the latent nuclear norm (Tomioka, Hayashi, and Kashima 2010; Signoretto et al. 2011; Liu et al. 2013).

Factorization methods, which represent the tensor as a product of smaller matrices and tensors, have also been used to learn low-rank tensors, popular examples are Tucker/CP decomposition (Kolda and Bader 2009) and tensor-train decomposition (Oseledets 2011). Compared with nuclear norm based methods, their optimization problems are not convex, thus are harder to optimize, and their empirical performance is often inferior than above convex ones (Tomioka et al. 2011; Liu et al. 2013; Guo, Yao, and Kwok 2017).

## 2.3 Proximal Average (PA) Algorithm

As the proposed algorithm is built on PA algorithm, we describe its details here. PG algorithms are efficient when the proximal step has the closed-form solution. However, in many cases, e.g., group/fused lasso (Jacob, Obozinski, and Vert 2009) and overlapped nuclear norm (Tomioka, Hayashi, and Kashima 2010), such requirement cannot be met. Generally, the optimization problem is formulated as

$$\min_{\mathbf{X}} f(\mathbf{X}) + \sum_{i=1}^K \lambda_i g_i(\mathbf{X}), \quad (6)$$

where  $g_i$ s are regularizers overlapping with each other.

The PA algorithm (Yu 2013) extends PG algorithm to problem (6). Let  $g \equiv \sum_{i=1}^K g_i$  and  $\mathbf{X}_t$  be current iterate.

Unlike the PG algorithm, which needs to compute  $\text{prox}_{\frac{\lambda}{\tau}\phi}(\cdot)$  in (4) with no closed-form solutions, PA algorithm generates  $\mathbf{X}_{t+1}$  via

$$\mathbf{Y}_{t+1}^i = \text{prox}_{\frac{\lambda_i}{\tau} g_i}(\mathbf{Z}_t), \quad \forall i = \{1, \dots, K\}, \quad (7)$$

$$\mathbf{X}_{t+1} = \sum_{i=1}^K \alpha_i \mathbf{Y}_{t+1}^i, \quad (8)$$

where  $\alpha_i = \lambda_i / \sum_{i=1}^K \lambda_i$ .

Usually, we have the closed-form solution on the proximal step with each individual  $g_i$  (but not for  $g$ ). Thus, PA algorithm can be significantly faster than PG algorithms, which has to iteratively and exactly solve the proximal step. Although the proximal step is only approximately solved, with a proper stepsize  $\rho$ , PA algorithm guarantees generating an optimal problem of (6) when both  $f$  and  $g$  are convex (Yu 2013). Recently, PA algorithm has also been extended for the nonconvex case, which allows both  $f$  and  $g_i$ s to be nonconvex. The requirements are  $f$  is Lipschitz smooth, and each  $g_i$  is continuous and can be decomposed as a difference of two convex functions (Zhong and Kwok 2014; Yu, Micol, and Xing 2015).

## 3 Proposed Algorithm

We focus on 3-order tensor in this paper. As mentioned above, we want to boost the performance of tensor completion by less penalizing top singular values. Motivated by the success of nonconvex regularization for learning low-rank matrices, we combine such nonconvex regularization with overlapped nuclear norm (Definition 1). Then, our tensor completion objective becomes

$$\min_{\mathbf{X}} F(\mathbf{X}) \equiv \frac{1}{2} \|P_{\Omega}(\mathbf{X} - \mathbf{O})\|_F^2 + \sum_{d=1}^D \lambda_d \phi(\mathbf{X}_{\langle d \rangle}). \quad (9)$$

Depending on applications, we can choose  $D = 2$  or 3 (see details in Section 4). Thus, the regularization here is slightly different from Definition 1, we may not need to add low-rank regularization to each unfolding matrix from  $\mathfrak{X}$ .

**Remark 3.1.** *When  $D = 1$ , (9) reduces to the matrix completion problem, which has been previously studied in (Lu et al. 2016; Yao et al. 2017b; Mazumder, Saldana, and Weng 2018) and can be solved by PG algorithms. However, when  $D = 2$  or 3, (9) is a tensor problem and PG algorithm cannot be applied.*

When  $\kappa(\alpha) = |\alpha|$ , (9) becomes a convex problem with the overlapped nuclear norm regularization. Algorithms, e.g., alternating direction of multiple multipliers (ADMM) (Tomioka, Hayashi, and Kashima 2010; Gandy, Recht, and Yamada 2011), and fast low-rank tensor completion (FaLRTC) (Liu et al. 2013), have been developed, which have the convergence guarantee. However, when the nonconvex regularization is used, neither of above two approaches can be applied. ADMM does not have the convergence guarantee in such a nonconvex case (Boyd et al. 2011), and FaLRTC fails due to the usage of the dual problem, which also relies on the convexity of the objective. Besides, algorithms for

the factorization-based tensor completion, such as gradient descent (Acar et al. 2011) and optimization on Riemannian manifold (Kasai and Mishra 2016), cannot be used either, as  $\mathcal{X}$  in (9) cannot be optimized based on tensor factorization.

### 3.1 Using PA Algorithm

While all previous algorithms considered by the literature of tensor completion (Song et al. 2017) fail on (9), here, we first observe PA algorithm, which is introduced in Section 2.3, can still be applied with the convergence guarantee. However, we will also show such a usage is far from the efficiency for real applications.

To apply PA algorithm, each nonconvex regularizer  $g_i$  needs to be Lipschitz continuous and admits a difference of convex decomposition (Zhong and Kwok 2014). For our problem (9), we have the following Proposition.

**Proposition 3.1.**  $\phi(\mathbf{X})$  is  $L$ -Lipschitz continuous, and admits a difference of convex decomposition.

Besides, the closed-form solution of nonconvex regularizer for each mode is offered in Lemma 2.1. Thus, let the current iterate be  $\mathcal{X}_t$ . According to (7)-(8), the next iterate  $\mathcal{X}_{t+1}$  in PA algorithm is generated as

$$\mathbf{Y}_{t+1}^i = \text{prox}_{\frac{\lambda_i}{\tau}\phi}([\mathcal{Z}_t]_{\langle i \rangle}), \quad \forall i = \{1 \dots D\}, \quad (10)$$

$$\mathcal{X}_{t+1} = \sum_{i=1}^D \alpha_i (\mathbf{Y}_{t+1}^i)_{\langle i \rangle}, \quad (11)$$

where

$$\mathcal{Z}_t = \mathcal{X}_t - \frac{1}{\tau} \nabla f(\mathcal{X}_t) = \mathcal{X}_t - \frac{1}{\tau} P_{\Omega}(\mathcal{X}_t - \mathbf{O}_t). \quad (12)$$

---

**Algorithm 1** PA algorithm (Zhong and Kwok 2014).

---

```

1: initialize  $\mathcal{X}_0 = 0$  and step-size  $\tau > \rho$ ;
2: for  $t = 1, \dots, T$  do
3:    $\mathcal{Z}_t = \mathcal{X}_t - \frac{1}{\tau} P_{\Omega}(\mathcal{X}_t - \mathbf{O})$ ;
4:   for  $i = 1, \dots, D$  do
5:      $\mathbf{Y}_{t+1}^i = \text{prox}_{\frac{\lambda_i}{\tau}\phi}([\mathcal{Z}_t]_{\langle i \rangle})$ ;
6:   end for
7:    $\mathcal{X}_{t+1} = \sum_{i=1}^D \alpha_i (\mathbf{Y}_{t+1}^i)_{\langle i \rangle}$ ;
8: end for
9: return  $\mathcal{X}_{T+1}$ .
```

---

The only difference between (7)-(8) and (10)-(11) are that extra folding/unfolding operations on  $\mathcal{Z}_t$  are needed. Thus, due to Proposition 3.1, (9) can already be solved by PA algorithm with the convergence guarantee (Zhong and Kwok 2014). Besides, as discussed above, it is the only choice for our problem (9). However, in the sequel, we will show such a direct usage is far from the efficiency. In real-world applications, images can have millions of pixels and the social network can have thousands of users. For these applications, we have following problems for PA algorithm (note that  $I_{\times}$  and  $I_{+}$  are defined in notation section):

(A). Large space: only  $O(\|\Omega\|_1)$  space is needed for training data, but  $O(I_{\times})$  space is required for PA algorithm due to the storage of  $\mathcal{X}_t$ ;

- (B). Expensive iterations: each iteration needs  $O(I_{\times} I_{+})$  time as SVD is needed in proximal steps in (10);
- (C). Slow convergence: PA algorithm is a plain first-order optimization algorithm, which can be slow to converge. Thus, many iterations may be needed.

In following Section 3.2, we show how the problem (A) and (B) can be solved based on one important proposition (Proposition 3.2) and then we fix the problem (C) in Section 3.3. A high level comparison of the proposed algorithm and the plain PA algorithm is at Table 2. Finally, the convergence of the proposed algorithm is in Section 3.4.

### 3.2 Solving the Computation Issue

In this section, we solve issue (A) and (B) simultaneously. The key is an important proposition preserves a special “sparse plus low-rank” structure for the proximal average step. Such structure comes from  $\mathcal{Z}_t$  (defined in (12)), which can be further expressed as

$$\mathcal{Z}_t = \sum_{i=1}^D \alpha_i (\mathbf{Y}_t^i)_{\langle i \rangle} - \frac{1}{\tau} P_{\Omega}(\mathcal{X}_t - \mathbf{O}_t), \quad (13)$$

where  $\sum_{i=1}^D \alpha_i (\mathbf{Y}_t^i)_{\langle i \rangle}$  is a mixture of low-rank matrices (with folding back to tensor); and  $\frac{1}{\tau} P_{\Omega}(\mathcal{X}_t - \mathbf{O}_t)$  is a sparse tensor. In this sense,  $\mathcal{Z}_t$  has a special “sparse plus low-rank” structure.

In the sequel, to show why such structure is important, we first show how the similar structure has been used for the low-rank matrix completion (Mazumder, Hastie, and Tibshirani 2010; Yao et al. 2017b). Then, we explain why these techniques cannot be transferred to tensor completion, which dues to folding/unfolding operations. Finally, we propose an important proposition which preserves the special structure and avoids above operations.

**Reducing to Matrix: The easiest case.** Let us consider the case  $D = 1$ . Then, (9) reduces from tensor to matrix problem (2) as  $\mathcal{X} = \mathbf{Y}_{\langle 1 \rangle}^1$ . “Sparse plus low-rank” structure has played an important role for the matrix completion (Mazumder, Hastie, and Tibshirani 2010; Yao et al. 2017b), we briefly recall how it can be used for here. In this case, iterates (10)-(11) becomes

$$\mathbf{Y}_{t+1}^1 = \text{prox}_{\frac{\lambda_1}{\tau}\phi}([\mathcal{Z}_t]_{\langle 1 \rangle}),$$

where

$$([\mathcal{Z}_t]_{\langle 1 \rangle}) = \mathbf{Y}_t^1 - \frac{1}{\tau} P_{\Omega_{\langle 1 \rangle}}(\mathbf{Y}_t^1 - \mathbf{O}_{\langle 1 \rangle}). \quad (14)$$

While SVD is needed to solve the proximal step, as mentioned in (Yao et al. 2017b), only a few top singular values of  $([\mathcal{Z}_t]_{\langle 1 \rangle})$  are needed. To compute them, one can use the power method (Halko, Martinsson, and Tropp 2011), then matrix multiplications of  $([\mathcal{Z}_t]_{\langle 1 \rangle}) \mathbf{v}$  for  $\mathbf{v} \in \mathbb{R}^{I_2 I_3}$  and  $(\mathbf{u}^{\top} [\mathcal{Z}_t]_{\langle 1 \rangle})$  for  $\mathbf{u} \in \mathbb{R}^{I_1}$  are needed. Let the rank of  $(\mathbf{Y}_t^1)_{\langle 1 \rangle}$  be  $k_t^1$ , and its factorization be  $\mathbf{U}_t^1 (\mathbf{V}_t^1)^{\top}$ . Using (14),  $([\mathcal{Z}_t]_{\langle 1 \rangle}) \mathbf{v}$  can be performed as

$$([\mathcal{Z}_t]_{\langle 1 \rangle}) \mathbf{v} = \mathbf{U}_t^1 ((\mathbf{V}_t^1)^{\top} \mathbf{v}) - \frac{1}{\tau} P_{\Omega_{\langle 1 \rangle}}(\mathbf{Y}_t^1 - \mathbf{O}_{\langle 1 \rangle}) \mathbf{v}, \quad (15)$$

Table 2: A comparison of PA algorithm with the proposed algorithm. Note that PA algorithm is the only existing solver for (9), which has convergence guarantee.

	Iteration complexity	Memory	Convergence
PA	$O(\sum_{i=1}^D I_i I_\times)$	$O(I_\times)$	slow
Ours	$O(\sum_{i=1}^D (I_\times/I_i + I_i) k_{t+1}^i k_t^i + \ \Omega\ _1 k_{t+1}^i)$	$O(\sum_{i=1}^D (I_\times/I_i + I_i) k_i^t + \ \Omega\ _1)$	fast

which takes  $O((I_1 + I_2 I_3) k_t^1 + \|\Omega\|_1)$  time (similarly for  $\mathbf{u}^\top(\mathcal{Z}_t)_{\langle 1 \rangle}$ ). As a low-rank tensor wants to be recovered, we can have  $k_t^1 \ll I_1$ . Thus, this is much faster than a direct multiplication of  $(\mathcal{Z}_t)_{\langle 1 \rangle} \mathbf{v}$ , which takes  $O(I_1 I_2 I_3)$  time. Assume there  $k_{t+1}$  singular values of  $(\mathcal{Z}_t)_{\langle 1 \rangle}$  are required to compute the proximal step, which is also the rank of  $(\mathcal{X}_{t+1})_{\langle 1 \rangle}$ . The proximal step takes  $O((I_1 + I_2 I_3) k_t^1 k_{t+1}^1 + \|\Omega\|_1 k_{t+1}^1)$  time, and is much cheaper than  $O(I_\times k_{t+1})$  time without utilizing the ‘‘sparse plus low-rank’’ structure.

Besides, we only need to keep the factorized form of  $\mathbf{Y}_t^1$ , and the space needed is cut down from  $O(I_\times)$  to  $O((I_1 + I_2 I_3) k_t^1 + \|\Omega\|_1)$ , which also becomes much smaller.

**Folding/Unfolding: The real problem.** When we have  $D = \{2, 3\}$ , the structure in (14) for the matrix cannot be used, as it is a tensor problem and the issue lies on folding/unfolding operations.

Again, we need to solve the proximal step in (10), which requires the matrix multiplication of  $(\mathcal{Z}_t)_{\langle i \rangle} \mathbf{v}$  and  $(\mathbf{u}^\top \mathcal{Z}_t)_{\langle i \rangle}$  for  $i = 1, \dots, D$ . Using  $(\mathcal{Z}_t)_{\langle i \rangle} \mathbf{v}$  for  $\mathbf{v} \in \mathbb{R}^{I_\times/I_i}$  as an example, from (13), we have

$$\begin{aligned} (\mathcal{Z}_t)_{\langle i \rangle} \mathbf{v} &= \left[ \sum_{j=1}^D \alpha_j (\mathbf{Y}_t^j)_{\langle j \rangle} \right]_{\langle i \rangle} \mathbf{v} - \frac{1}{\tau} [P_\Omega(\mathcal{X}_t - \mathcal{O}_t)]_{\langle i \rangle} \mathbf{v} \\ &= \alpha_i \mathbf{U}_t^i [(\mathbf{V}_t^i)^\top \mathbf{v}] + \left[ \sum_{j \neq i} \alpha_j (\mathbf{U}_t^j (\mathbf{V}_t^j)^\top)_{\langle j \rangle} \right]_{\langle i \rangle} \mathbf{v} \\ &\quad - \frac{1}{\tau} [P_\Omega(\mathcal{X}_t - \mathcal{O}_t)]_{\langle i \rangle} \mathbf{v}, \end{aligned} \quad (16)$$

where  $\mathbf{U}_t^i (\mathbf{V}_t^i)^\top$  is the factorized form of  $\mathbf{Y}_t^i$ . Comparing with (15), while the first term in (16) can be directly computed with matrix multiplications, the second term involves with folding and unfolding along different mode of tensor, and the sparse tensor in the third term also needs the unfolding operation. The same holds for  $\mathbf{u}^\top(\mathcal{Z}_t)_{\langle i \rangle}$  with  $\mathbf{u} \in \mathbb{R}^{I_i}$ , which can be seen from

$$\begin{aligned} \mathbf{u}^\top(\mathcal{Z}_t)_{\langle i \rangle} &= \alpha_i (\mathbf{u}^\top \mathbf{U}_t^i) (\mathbf{V}_t^i)^\top + \mathbf{u}^\top \left[ \sum_{j \neq i} \alpha_j (\mathbf{U}_t^j (\mathbf{V}_t^j)^\top)_{\langle j \rangle} \right]_{\langle i \rangle} \\ &\quad - \frac{1}{\tau} \mathbf{u}^\top [P_\Omega(\mathcal{X}_t - \mathcal{O}_t)]_{\langle i \rangle}. \end{aligned} \quad (17)$$

If these folding/unfolding problems are not solved, we have to explicitly get the full tensor  $\mathcal{Z}_t$ , which still leads to the space requirement of  $O(I_\times)$  and the iteration time complexity of  $O(\sum_{i=1}^D k_t^i I_\times)$  where  $k_t^i$  is the rank of  $(\mathcal{X}_t)_{\langle i \rangle}$ . Such complexities are the same as the direct usage of PA algorithm (Table 2), and the ‘‘special structure’’ becomes usefulness here.

**Solving the Problem.** Here, we solve the problem raising from folding and unfolding. For the low-rank part, i.e.,  $\left[ \sum_{j \neq i} \alpha_j (\mathbf{U}_t^j (\mathbf{V}_t^j)^\top)_{\langle j \rangle} \right]_{\langle i \rangle} \mathbf{v}$  in (16) and

$\mathbf{u}^\top \left[ \sum_{j \neq i} \alpha_j (\mathbf{U}_t^j (\mathbf{V}_t^j)^\top)_{\langle j \rangle} \right]_{\langle i \rangle}$  in (17), where we need to folding a low-rank matrix along with  $j$ th mode and unfold on  $i$ th mode, we make use of following Proposition 3.2.

**Proposition 3.2.** *Let  $\{\pi_1, \pi_2, \pi_3\}$  be any permutation of  $\{1, 2, 3\}$ ,  $\mathbf{A} \in \mathbb{R}^{I_{\pi_1} \times k}$  and  $\mathbf{B} \in \mathbb{R}^{I_{\pi_2} I_{\pi_3} \times k}$ , and  $\mathbf{a}_p$  (resp.  $\mathbf{b}_p$ ) is the  $p$ th column in  $\mathbf{A}$  (resp.  $\mathbf{B}$ ). For any  $\mathbf{u} \in \mathbb{R}^{I_{\pi_1}}$  and  $\mathbf{v} \in \mathbb{R}^{I_{\pi_2} I_{\pi_3}}$ , we have*

$$\begin{aligned} \mathbf{u}^\top \left( (\mathbf{A}\mathbf{B}^\top)_{\langle \pi_1 \rangle} \right)_{\langle \pi_2 \rangle} &= \sum_{p=1}^k \mathbf{a}_p^\top \otimes (\mathbf{u}^\top \text{mat}(\mathbf{b}_p)), \\ \left( (\mathbf{A}\mathbf{B}^\top)_{\langle \pi_1 \rangle} \right)_{\langle \pi_2 \rangle} \mathbf{v} &= \sum_{p=1}^k \text{mat}(\mathbf{b}_p) \text{mat}(\mathbf{v})^\top \mathbf{a}_p, \end{aligned}$$

where  $\otimes$  denotes Kronecker product, and  $\text{mat}(\mathbf{c})$  reshapes a vector  $\mathbf{c} \in \mathbb{R}^{I_{\pi_2} I_{\pi_3}}$  to a  $I_{\pi_2} \times I_{\pi_3}$  matrix.

Thus, no folding and unfolding are required and the multiplications of above low-rank parts only needs  $O(\sum_{j \neq i} k_t^i (I_\times/I_i + I_i))$  instead of  $O(\sum_{i=1}^D k_t^i I_\times)$  time. Besides, the space requirement is also cut down from  $O(I_\times)$  to  $O(\sum_{j \neq i} (I_\times/I_i + I_i) k_t^i)$ . The above Proposition are new for the literature of tensor completion, and cannot be derived from previous papers for the matrix case (Mazumder, Hastie, and Tibshirani 2010; Yao et al. 2017b) either.

Next, for the sparse part, i.e.  $[P_\Omega(\mathcal{X}_t - \mathcal{O}_t)]_{\langle i \rangle} \mathbf{v}$  in (16) and  $\mathbf{u}^\top [P_\Omega(\mathcal{X}_t - \mathcal{O}_t)]_{\langle i \rangle}$  in (17). As  $P_\Omega(\mathcal{X}_t - \mathcal{O}_t)$  is a sparse tensor, we only need to keep track of the observed positions in  $\Omega$ . We use the coordinate format here, as it is the most popularly used format for sparse tensors. There are other possible formats for storing a sparse tensor, however, due to multiple orders of the tensor, they are not as efficient as the coordinate format (Bader and Kolda 2007). We focus on 3-order tensor in this paper. In this case, coordinate format represents the  $j$ th observed element in the sparse tensor as  $\{i_p^1, i_p^2, i_p^3, v_p\}$ , where  $\{i_p^1, i_p^2, i_p^3\}$  are the index on each mode and  $v_p$  is the value.

To construct  $P_\Omega(\cdot)$ , we need to first compute  $P_\Omega(\mathcal{X}_t)$ . Given factorized forms of  $\mathbf{Y}^i$ s, each observed element in  $P_\Omega(\mathcal{X}_t)$  can be computed with Algorithm 2 (step 5-6 are not need if  $D = 2$  is used). Thus, its construction takes  $O(\|\Omega\|_1 \sum_{i=1}^D k^i)$  time. After this, existing packages for sparse tensors can be reused for computing

$[P_\Omega(\mathbf{X}_t - \mathbf{O}_t)]_{\langle i \rangle} \mathbf{v}$  and  $\mathbf{u}^\top [P_\Omega(\mathbf{X}_t - \mathbf{O}_t)]_{\langle i \rangle}$  (Bader and Kolda 2007), which takes  $O(\|\Omega\|_1)$  space and time.

---

**Algorithm 2** Compute the  $p$ th element in  $P_\Omega(\mathbf{X})$ .

---

**Require:** index  $\{i_p^1, i_p^2, i_p^3\}$ , factorization of  $\mathbf{Y}^1, \mathbf{Y}^2, \mathbf{Y}^3$ ;

- 1:  $\mathbf{u}_1$ : the  $i_p^1$ th row of  $\mathbf{U}^1$ ;
- 2:  $\mathbf{v}_1$ : the  $(i_p^2 I_2 + i_p^3)$ th row of  $\mathbf{V}^1$ ;
- 3:  $\mathbf{u}_2$ : the  $i_p^2$ th row of  $\mathbf{U}^2$ ;
- 4:  $\mathbf{v}_2$ : the  $(i_p^3 I_3 + i_p^1)$ th row of  $\mathbf{V}^2$ ;
- 5:  $\mathbf{u}_3$ : the  $i_p^3$ th row of  $\mathbf{U}^3$ ;
- 6:  $\mathbf{v}_3$ : the  $(i_p^1 I_1 + i_p^2)$ th row of  $\mathbf{V}^3$ ;
- 7: **return**  $v_p = \sum_{i=1}^3 \alpha_i \mathbf{u}_i^\top \mathbf{v}_i$

---

As a result, the multiplications of (16) and (17) can be done in  $O(\sum_{i=1}^D (I_\times / I_i + I_i) k_t^i + \|\Omega\|_1)$  space and time. This makes the usage of special “sparse plus low-rank” structure in  $\mathbf{Z}_t$  become significant here.

It is ready to plug techniques proposed here into Algorithm 1, and then issue (A) and (B) are being solved. As  $D$  proximal steps are needed in step 5, the resulting algorithm has the iteration time complexity of  $O(\sum_{i=1}^D k_t^i k_{t+1}^i (I_\times / I_i + I_i) + k_{t+1}^i \|\Omega\|_1)$  and space requirement of  $O(\|\Omega\|_1 + \sum_{i=1}^D (I_\times / I_i + I_i) k_t^i)$ .

### 3.3 Speedup Convergence

Recall that the running time depends on the product of iteration time complexity and the total number of iterations. The PA algorithm is still based on the first-order approach, which usually suffers from the slow convergence (issue (C)) (Parikh and Boyd 2013), and many iterations are needed. We have made iteration much cheaper in Section 3.2, here we cut down total iterations of PA algorithm.

We solve this issue by adopting the Nesterov acceleration (Nesterov 1983). The proposed tensor completion with non-convex regularization (TCNR) algorithm is in Algorithm 3. Compared with Algorithm 1, the acceleration is done in step 3 ( $F_\tau$  is defined in Lemma 3.3). Then, to ensure convergence, an extra check on the object value is in step 4. If the interpolated point  $\mathbf{Y}_t$  is better than  $\mathbf{X}_t$ , then we do the proximal step with  $\mathbf{Y}_t$ , otherwise,  $\mathbf{Y}_t$  is not accepted and the proximal step is done with  $\mathbf{X}_t$ . Note that, no tensors need to be explicitly formed during iterating. On running time, using techniques in Section 3.2, we only need to keep sparse tensors  $P_\Omega(\cdot)$  and factorized form of  $\mathbf{Y}_t^i$ . Besides, while  $\mathbf{Y}_t$  is more complex than  $\mathbf{X}_t$ , the special “sparse plus low-rank” structure still exists for the proximal step with  $\mathbf{Y}_t$  (see details in Appendix B).

Compared with no usage of the acceleration, the iteration time and complexity of Algorithm 3 is slightly higher, but still in  $O(\sum_{i=1}^D r_t^i k_t^i (I_\times / I_i + I_i) + r_t^i \|\Omega\|_1)$  and  $O(\|\Omega\|_1 + \sum_{i=1}^D (I_\times / I_i + I_i) k_t^i)$  respectively.

**Remark 3.2.** Nesterov acceleration is a popular trick to address this issue, which has been recently adopted in PG algorithm (Li 2015; Yao et al. 2017a; Ghadimi and Lan 2016). However, PA algorithm solves different problems

---

**Algorithm 3** Tensor Completion with Nonconvex Regularization (TCNR) algorithm.

---

- 1: initialize  $\mathbf{X}_0 = \mathbf{X}_1 = 0$  and step-size  $\tau > (\rho + DL)$ ;
- 2: **for**  $t = 1, \dots, T$  **do**
- 3:    $\mathbf{Y}_t = \mathbf{X}_t + \frac{t-1}{t+2} (\mathbf{X}_t - \mathbf{X}_{t-1})$ ;
- 4:   **if**  $F_\tau(\mathbf{Y}_t) \leq F_\tau(\mathbf{X}_t)$  **then**
- 5:      $\mathbf{V}_t = \mathbf{Y}_t$ ;
- 6:   **else**
- 7:      $\mathbf{V}_t = \mathbf{X}_t$ ;
- 8:   **end if**
- 9:    $\mathbf{Z}_t = \mathbf{V}_t - \frac{1}{\tau} P_\Omega(\mathbf{V}_t - \mathbf{O})$ ;
- 10:   **for**  $i = 1, \dots, D$  **do**
- 11:      $\mathbf{X}_{t+1}^i = \text{prox}_{\frac{\lambda_i}{\tau} \kappa}((\mathbf{Z}_t)_{\langle i \rangle})$ ;
- 12:   **end for**
- 13:    $\mathbf{X}_{t+1} = \sum_{i=1}^D \alpha_i (\mathbf{X}_{t+1}^i)_{\langle i \rangle}$ ; // construct implicitly
- 14: **end for**
- 15: **return**  $\mathbf{X}_{T+1}$ .

---

compared with PG algorithm, i.e., (6) v.s. (2), and the acceleration has not been done with PA algorithm for the nonconvex optimization yet.

### 3.4 Convergence Analysis

Before discussing the convergence, we first show in Lemma 3.3 that PA algorithm actually optimizes an approximate regularizer.

**Lemma 3.3** ((Zhong and Kwok 2014)). *There exists a function  $\bar{g}_\tau$ , such that  $\text{prox}_{\bar{g}_\tau}(\mathbf{Z}) = \sum_{i=1}^D \alpha_i \text{prox}_{\frac{\lambda_i}{\tau} \phi}([\mathbf{Z}]_{\langle i \rangle})$  for any  $\tau > 0$ .*

Let  $F_\tau(\mathbf{X}) \equiv \frac{1}{2} \|P_\Omega(\mathbf{X} - \mathbf{O})\|_F^2 + \bar{g}_\tau(\mathbf{X})$ . However, the difference of the original problem  $F$  and  $F_\tau$  can be bounded in Proposition 3.4.

**Proposition 3.4.**  $0 \leq \min F - \min F_\tau \leq \frac{1}{\tau} \sum_{i=1}^D \alpha_i L^2$ .

The convergence of Algorithm 3 is in Theorem 3.5.

**Theorem 3.5.** *The sequence  $\{\mathbf{X}_t\}$  generated from Algorithm 3 has at least one limit point, and all limit points are also critical points of  $F_\tau(\mathbf{X})$ .*

Together with Proposition 3.4, we can see that the larger  $\tau$  leads to the better approximation to the original problem  $F$ . However, it also leads to the smaller steps, which makes the convergence slower. In experiments, we empirically take  $\tau = 1$ . Besides, since  $F_\tau$  is hard to evaluate, we use  $F$  instead as suggested by (Zhong and Kwok 2014).

**Remark 3.3.** *Previous proofs cannot be directly used, as they do not consider the proximal average (Li 2015; Yao et al. 2017a; Ghadimi and Lan 2016) or assume the objective is convex (Yu 2013), or do not use the acceleration (Zhong and Kwok 2014; Yu, Micol, and Xing 2015). While no rate is given by Theorem 3.5, it empirically give significant speed up over its non-accelerated variants. This is also previously observed for PG algorithms on learning sparse vectors (Li 2015) and low-rank matrices (Yao et al. 2017b). Moreover, the faster rate resulting from the acceleration*

Table 3: Recovery performance of various algorithms on synthetic data (Case (i)). The lowest and comparable RMSEs (according to the pairwise t-test with 95% confidence) are highlighted.

Case (i)		$c = 250$ , sparsity: 10.22%		$c = 500$ , sparsity: 5.64%		$c = 1000$ , sparsity: 3.09%	
		RMSE	rank	RMSE	rank	RMSE	rank
convex	PA-APG	0.0137±0.0008	157,156	0.0141±0.0012	211,211	0.0149±0.0011	184.183
nonconvex (capped- $\ell_1$ )	GDPAN	<b>0.0102±0.0001</b>	5,5	<b>0.0103±0.0001</b>	5,5	<b>0.0103±0.0001</b>	5,5
	TCNR(w/o-acc)	<b>0.0102±0.0001</b>	5,5	<b>0.0103±0.0001</b>	5,5	<b>0.0103±0.0001</b>	5,5
	TCNR-acc	0.0103±0.0001	5,5	<b>0.0103±0.0001</b>	5,5	<b>0.0103±0.0001</b>	5,5
nonconvex (LSP)	GDPAN	0.0103±0.0001	5,5	<b>0.0103±0.0001</b>	5,5	0.0104±0.0001	5,5
	TCNR(w/o-acc)	0.0103±0.0001	5,5	<b>0.0103±0.0001</b>	5,5	0.0104±0.0001	5,5
	TCNR-acc	0.0103±0.0001	5,5	<b>0.0103±0.0001</b>	5,5	0.0104±0.0001	5,5
nonconvex (TNN)	GDPAN	0.0103±0.0001	5,5	0.0104±0.0001	5,5	0.0104±0.0001	5,5
	TCNR(w/o-acc)	0.0103±0.0001	5,5	0.0104±0.0001	5,5	0.0104±0.0001	5,5
	TCNR-acc	<b>0.0102±0.0001</b>	5,5	0.0104±0.0001	5,5	<b>0.0103±0.0001</b>	5,5

Table 4: CPU time (seconds) of various algorithms on synthetic data (Case (i) and (ii)). The shortest CPU time (according to the pairwise t-test with 95% confidence) are highlighted.

		Case (i).			Case (ii).		
		$c = 250$	$c = 500$	$c = 1000$	$c = 100$	$c = 200$	$c = 400$
convex	PA-APG	30.6±9.6	257.2±34.8	2131.7±419.9	13.0±2.4	250.1±59.6	6196.4±2033.4
nonconvex (capped- $\ell_1$ )	GDPAN	20.6±15.5	64.4±29.5	665.4±99.8	15.8±3.8	179.9±21.5	3670.4±225.8
	TCNR(w/o-acc)	4.2±2.8	7.1±4.5	27.9±5.1	4.2±2.1	22.9±1.1	575.9±70.9
	TCNR	<b>1.0±0.4</b>	<b>2.1±1.4</b>	<b>5.9±1.6</b>	1.1±0.5	5.1±0.3	89.4±13.4
nonconvex (LSP)	GDPAN	18.9±14.7	59.1±26.4	654.1±214.7	16.5±3.3	177.8±16.4	3794.0±419.5
	TCNR(w/o-acc)	3.9±3.0	4.5±1.5	27.9±5.7	3.2±0.4	21.8±0.8	544.2±75.5
	TCNR	<b>0.8±0.5</b>	<b>1.6±1.1</b>	<b>5.8±2.8</b>	1.1±0.2	4.6±0.7	81.3±24.9
nonconvex (TNN)	GDPAN	19.2±14.6	69.3±26.4	615.0±140.9	19.0±3.6	184.1±17.7	3922.9±280.1
	TCNR(w/o-acc)	8.2±8.8	6.6±3.8	26.2±4.0	3.4±0.8	21.8±0.9	554.7±44.1
	TCNR	<b>0.8±0.3</b>	<b>1.4±0.3</b>	<b>5.3±1.5</b>	1.0±0.2	4.8±0.4	78.0±9.4

for the nonconvex problem is still an open issue (Li 2015; Ghadimi and Lan 2016).

## 4 Experiments

Experiments are performed on a PC with Intel i7 CPU and 32GB memory. All algorithms are implemented in Matlab, except operations on sparse tensor and matrix are implemented in C and linked to Matlab by mex files.

### 4.1 Synthetic Data

In the synthetic data, we consider two cases, i.e.,  $D = 2$  and 3 in (9). Note that no matter  $D = 2$  or 3, (9) is a tensor completion problem and cannot reduce to a matrix one. The difference is that, when  $D = 2$ , the low-rank regularizations are imposed on the first two unfolding matrices from  $\mathcal{X}$  but not the third one. The difference between  $D = 2$  and 3 is analyzed at the end of this sub-section.

We focus on comparing different variants of PA algorithm for the overlapped regularization, as PA algorithm is the only algorithm solving (9) with convergence guarantee. Thus, the following algorithms are compared

- GDPAN (Zhong and Kwok 2014): nonconvex PA algorithm (Algorithm 1);
- The proposed Algorithm 3 (denoted as TCNR), which utilizing acceleration and the “sparse plus low-rank” structure in computing the proximal step and its variant without acceleration (denoted as TCNR(w/o-acc)); and

- PA-APG (Yu 2013): accelerated PA algorithm for the convex overlapped nuclear norm is also included as a baseline.

All algorithms are stopped when the relative changes on the objective value is smaller than  $10^{-4}$ .

We consider three nonconvex penalties as examples here, capped- $\ell_1$  norm (Zhang 2010a), LSP (Candès, Wakin, and Boyd 2008) and TNN (Hu et al. 2013). Following (Lu et al. 2016; Yao et al. 2017b; 2017a), the recovery performance is measured by (i) root-mean-square-error (RMSE):

$$\text{RMSE} = \|\|P_{\bar{\Omega}}(\mathcal{X} - \bar{\mathcal{O}})\|_F / \sqrt{\|\bar{\Omega}\|_1},$$

where  $\mathcal{X}$  is the low-rank tensor recovered from different algorithms, and  $\bar{\Omega}$  denotes the unobserved elements in  $\bar{\mathcal{O}}$ ; (ii). running CPU time; and (iii). rank on each mode.

**Case (i): Small  $I_3$ .** We follow the setup suggested in (Song et al. 2017). The synthetic data is generated as  $\bar{\mathcal{O}} = \sum_{i=1}^5 s_i (\mathbf{a}_i \circ \mathbf{b}_i \circ \mathbf{c}_i)$ <sup>1</sup> where  $\mathbf{a}_i \in \mathbb{R}^{25c}$ ,  $\mathbf{b}_i \in \mathbb{R}^{25c}$  and  $\mathbf{c}_i \in \mathbb{R}^5$ . All the elements in  $\mathbf{a}_i$ s,  $\mathbf{b}_i$ s,  $\mathbf{c}_i$ s and  $s_i$ s are sampled independently from Gaussian distribution  $\mathcal{N}(0, 1)$ . A total number of  $\|\bar{\Omega}\|_1 = 5(50c + 5) \log(50c + 5)$  elements are uniform randomly observed from  $\bar{\mathcal{O}} = \bar{\mathcal{O}} + \mathcal{N}$ , where  $\mathcal{N}$  is the noise sampled independently from  $\mathcal{N}(0, 0.01)$ . We vary  $c = \{10, 20, 40\}$ . We use 50% of the observations for

<sup>1</sup>We follow (Kolda and Bader 2009), and  $\circ$  denotes out products with  $[\mathbf{a} \circ \mathbf{b} \circ \mathbf{c}]_{ijk} = a_i b_j c_k$ .

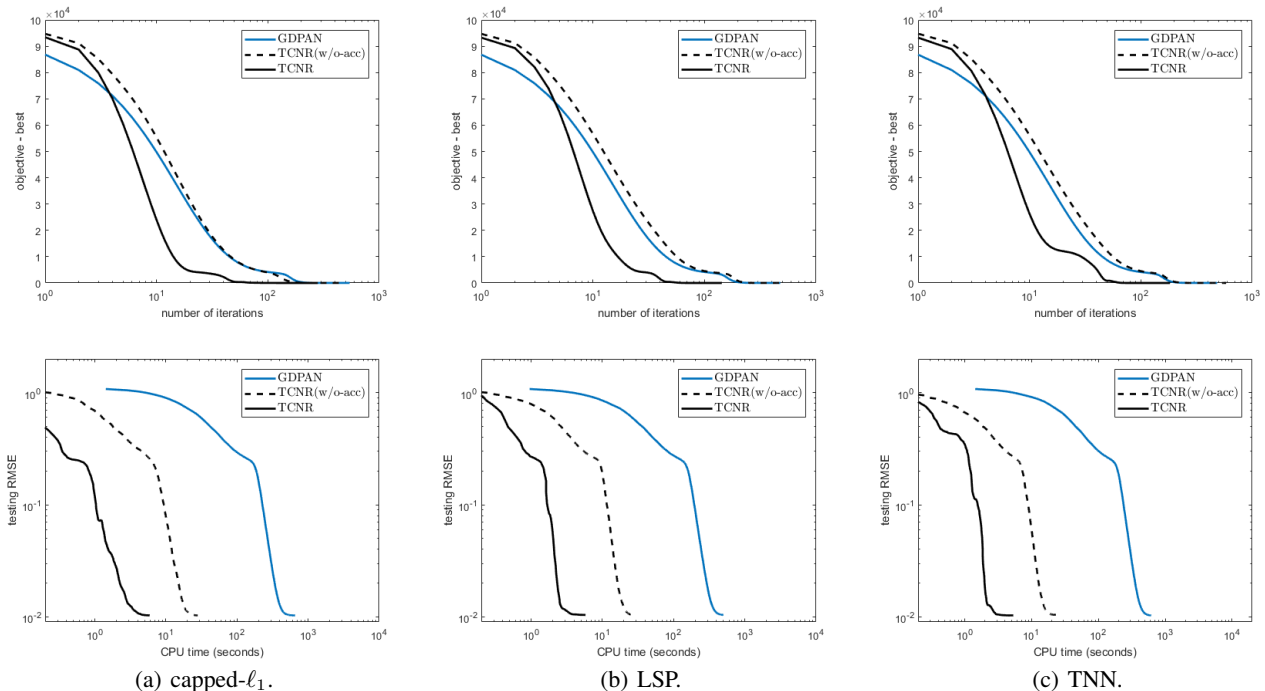


Figure 1: Convergence of testing RMSE on synthetic data (Case (i)) and  $c = 1000$ . Top: objective v.s. number of iterations; bottom: testing RMSE v.s. CPU time.

Table 5: Recovery performance of various algorithms on synthetic data (Case (ii)). The lowest and comparable RMSEs (according to the pairwise t-test with 95% confidence) are highlighted.

Case (ii)		$c = 100$ , sparsity:8.29%		$c = 200$ , sparsity:5.64%		$c = 400$ , sparsity:3.09%	
		RMSE	rank	RMSE	rank	RMSE	rank
convex	PA-APG	$0.0115 \pm 0.0016$	100,100,100	$0.0110 \pm 0.0007$	200,200,200	$0.0098 \pm 0.0001$	400,400,400
nonconvex (capped- $\ell_1$ )	GDPAN	<b><math>0.0015 \pm 0.0001</math></b>	5,5,5	<b><math>0.0010 \pm 0.0001</math></b>	5,5,5	<b><math>0.0006 \pm 0.0001</math></b>	5,5,5
	TCNR(w/o-acc)	<b><math>0.0015 \pm 0.0001</math></b>	5,5,5	<b><math>0.0010 \pm 0.0001</math></b>	5,5,5	<b><math>0.0006 \pm 0.0001</math></b>	5,5,5
	TCNR	<b><math>0.0015 \pm 0.0001</math></b>	5,5,5	<b><math>0.0009 \pm 0.0001</math></b>	5,5,5	<b><math>0.0006 \pm 0.0001</math></b>	5,5,5
nonconvex (LSP)	GDPAN	<b><math>0.0015 \pm 0.0001</math></b>	5,5,5	<b><math>0.0010 \pm 0.0001</math></b>	5,5,5	<b><math>0.0006 \pm 0.0001</math></b>	5,5,5
	TCNR(w/o-acc)	<b><math>0.0015 \pm 0.0001</math></b>	5,5,5	<b><math>0.0010 \pm 0.0001</math></b>	5,5,5	<b><math>0.0006 \pm 0.0001</math></b>	5,5,5
	TCNR	<b><math>0.0015 \pm 0.0001</math></b>	5,5,5	<b><math>0.0010 \pm 0.0001</math></b>	5,5,5	<b><math>0.0006 \pm 0.0001</math></b>	5,5,5
nonconvex (TNN)	GDPAN	<b><math>0.0015 \pm 0.0001</math></b>	5,5,5	<b><math>0.0010 \pm 0.0001</math></b>	5,5,5	<b><math>0.0006 \pm 0.0001</math></b>	5,5,5
	TCNR(w/o-acc)	<b><math>0.0015 \pm 0.0001</math></b>	5,5,5	<b><math>0.0010 \pm 0.0001</math></b>	5,5,5	<b><math>0.0006 \pm 0.0001</math></b>	5,5,5
	TCNR	<b><math>0.0015 \pm 0.0001</math></b>	5,5,5	<b><math>0.0010 \pm 0.0001</math></b>	5,5,5	<b><math>0.0006 \pm 0.0001</math></b>	5,5,5

training, the remained 50% for validation, and the testing is performed on the remain unobserved elements in  $\bar{\mathcal{O}}$ .

Experiments are repeated five times. Recovery performance is in Table 3. We can see that PA-APG, which is based on the convex overlapping nuclear norm, has much higher testing RMSEs than, GDPAN, TCNR(w/o-acc) and TCNR, which are based on the nonconvex regularization. Besides, three nonconvex penalties, i.e., capped- $\ell_1$ , LSP and TNN, have the similar empirical performance. This is also observed in (Lu et al. 2016; Yao et al. 2017a; 2017b; Mazumder, Saldana, and Weng 2018). Finally, GDPAN, TCNR(w/o-acc) and TCNR all identify the ground-truth rank, while the rank recovered by PA-APG is much higher.

The CPU time is in Table 4, and the convergence of testing RMSE and objective value are in Figure 1. First, we can see that both PA-APG and GDPAN are very slow. Then,

when measured by the number of iterations, TCNR(w/o-acc) converges as fast as GDPAN. However, when measured by CPU time, TCNR(w/o-acc) becomes much faster than GDPAN, as it utilizes the special “sparse plus low-rank” structure on computing the proximal steps. TCNR is even faster than TCNR(w/o-acc) due to acceleration.

**Case (ii): Large  $I_3$ .** The data are generated using the same method as the case  $D = 2$  but with  $I_1 = I_2 = I_3 = c$ , the same measurements and setup are also used. However,  $D = 3$  here, which means all three unfolding matrices are regularized now. Again, PA-APG, GDPAN, TCNR(w/o-acc) and TCNR, are compared.

Experiments are repeated five times. Results are in Table 5. Again, we can see three nonconvex regularizers, capped- $\ell_1$  norm, LSP and TNN, have the same testing RMSE. GDPAN, TCNR(w/o-acc) and TCNR, all have much



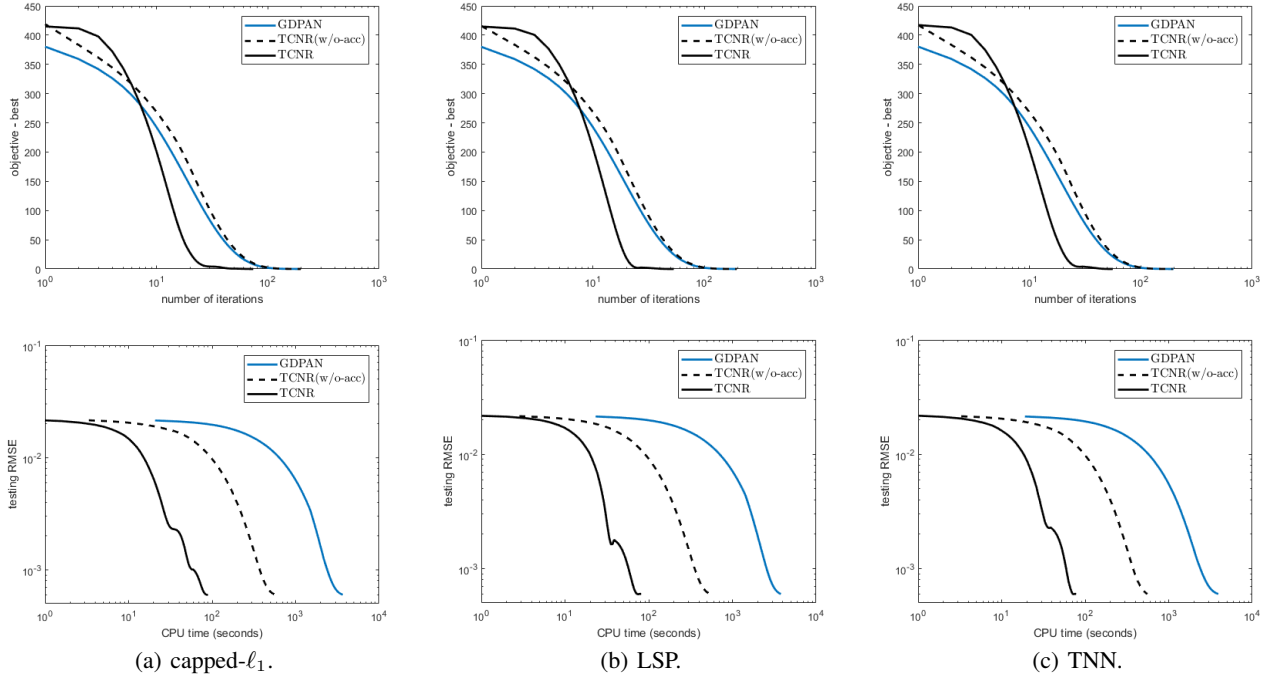


Figure 2: Convergence of testing RMSE on synthetic data (Case (ii)) with  $c = 400$ .

lower testing RMSEs than PA-APG, and identify the correct rank of the tensor. The CPU time is in Table 4, and convergence of testing RMSE and objective value are in Figure 2. Again, GDPAN is much slower than TCNR(w/o-acc) and TCNR. Besides, TCNR is the fastest due to utilization of special structure and acceleration.

**Comparison of Case (i) and (ii).** Finally, in this section, we examine the difference of  $D = 2$  and  $3$  in (9) on above two cases (Case (i) and (ii)). Only TCNR is considered here, and we use the superscript indicates the value of  $D$ .

The performance is compared in Table 6 for Case (i). We can see that TCNR<sup>2</sup> and TCNR<sup>3</sup> can achieve the same testing RMSEs. However, TCNR<sup>3</sup> is much slower than TCNR<sup>2</sup>. This dues to  $I_3$  is small, the low-rank assumption cannot hold on the third mode and  $k_3^t \ll I_3$  does not hold. Thus, the proximal step for the third mode (i.e.,  $i = 3$  for step 11 in Algorithm 3) is much more expensive than these for the first two modes.

Table 6 shows the comparison for Case (ii). On CPU time, as TCNR<sup>3</sup> has one more low-rank regularization than TCNR<sup>2</sup>, it is still more expensive. However, we have  $k_3^t \ll I_3$  in this case, proximal steps on all three modes take nearly the same amount of time. Thus, TCNR<sup>3</sup> is only slightly slower than TCNR<sup>2</sup>. On testing RMSE, the performance obtained from TCNR<sup>2</sup> is much worse than TCNR<sup>3</sup>, which results from TCNR<sup>2</sup> cannot capture the low-rank property on the third mode.

As a result, if  $I_3$  is small (Case (i)), we can just take  $D = 2$  in (9), which is very efficient and offers good performance. However, when  $I_3$  becomes large (Case (ii)), the low-rank regularization on the third mode is important, using  $D = 3$  in (9) is suggested.

## 4.2 Real Data sets

In the sequel, based on observations in synthetic cases, we use  $D = 2$  in (9) if  $I_3$  is very small (i.e.,  $I_3 \leq 10$  empirically), otherwise we use  $D = 3$ ; besides, as all three nonconvex penalty functions have similar performance, only LSP is considered.

**Color Image.** We use the same “Window” image (Figure 3) as (Guo, Yao, and Kwok 2017),<sup>2</sup> The summary of compared algorithms are in Table 8. For TMac-TT, there are too many ways to decompose a tensor into the tensor train format, we use the decomposition size of  $10 \times 10 \times 10 \times 10 \times 10 \times 10 \times 3$  as suggested by (Bengua et al. 2017).

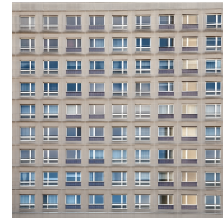


Figure 3: Color image “Window” ( $1000 \times 1000 \times 3$ ).

We normalize each pixels into range  $[0, 1]$ . We randomly sample 10% of all the pixels for training, and add Gaussian noise  $\mathcal{N}(0, 0.01)$  to them. Half of the ratings for training are used for validation. The rest unseen clean pixels are used for testing. Performance of various algorithms are measured by RMSE on the testing pixels and the CPU time.

<sup>2</sup>Note that the original image is of size  $3000 \times 2901 \times 3$ , we resize the image is of size  $1000 \times 1000 \times 3$  here in order to make a decomposition for TMac-TT algorithm.

Table 6: Comparisons of RMSEs on the synthetic data (Case (i)) with a different  $D$  used in TCNR. The CPU time is in seconds. The best and comparable performances (according to the pairwise t-test with 95% confidence) are highlighted.

Case (i)		$c = 250$		$c = 500$		$c = 1000$	
		RMSE	time (sec)	RMSE	time (sec)	RMSE	time (sec)
capped- $\ell_1$	TCNR <sup>2</sup>	0.0103±0.0001	<b>1.0±0.4</b>	<b>0.0103±0.0001</b>	<b>2.1±1.4</b>	<b>0.0103±0.0001</b>	<b>5.9±1.6</b>
	TCNR <sup>3</sup>	<b>0.0101±0.0001</b>	10.4±6.3	<b>0.0102±0.0001</b>	63.7±21.3	<b>0.0103±0.0001</b>	918.7±500.9
LSP	TCNR <sup>2</sup>	0.0103±0.0001	<b>0.8±0.5</b>	<b>0.0103±0.0001</b>	<b>1.6±1.1</b>	0.0104±0.0001	<b>5.8±2.8</b>
	TCNR <sup>3</sup>	0.0103±0.0001	6.7±2.2	<b>0.0102±0.0001</b>	50.1±8.8	<b>0.0103±0.0001</b>	899.7±404.4
TNN	TCNR <sup>2</sup>	<b>0.0102±0.0001</b>	<b>0.8±0.3</b>	0.0104±0.0001	<b>1.4±0.3</b>	<b>0.0103±0.0001</b>	<b>5.3±1.5</b>
	TCNR <sup>3</sup>	<b>0.0102±0.0002</b>	8.3±1.0	0.0104±0.0001	78.8±18.9	0.0104±0.0001	615.5±388.3

Table 7: Comparisons of RMSEs on the synthetic data (Case (ii)) with a different  $D$  used in TCNR. The CPU time is in seconds. The best and comparable performances (according to the pairwise t-test with 95% confidence) are highlighted.

Case (ii)		$c = 100$		$c = 200$		$c = 400$	
		RMSE	time (sec)	RMSE	time (sec)	RMSE	time (sec)
capped- $\ell_1$	TCNR <sup>2</sup>	0.0022±0.0001	<b>0.5±0.1</b>	0.0015±0.0001	<b>3.3±0.4</b>	0.0009±0.0001	<b>40.0±1.9</b>
	TCNR <sup>3</sup>	<b>0.0015±0.0001</b>	1.1±0.2	<b>0.0009±0.0001</b>	5.1±0.3	<b>0.0006±0.0001</b>	89.4±13.4
LSP	TCNR <sup>2</sup>	0.0022±0.0001	<b>0.7±0.2</b>	0.0014±0.0001	<b>3.3±0.4</b>	0.0010±0.0001	<b>50.8±27.2</b>
	TCNR <sup>3</sup>	<b>0.0015±0.0001</b>	1.1±0.2	<b>0.0010±0.0001</b>	4.6±0.7	<b>0.0006±0.0001</b>	81.3±24.9
TNN	TCNR <sup>2</sup>	0.0022±0.0001	<b>0.6±0.1</b>	0.0014±0.0001	<b>3.0±0.5</b>	0.0009±0.0001	<b>39.3±14.3</b>
	TCNR <sup>3</sup>	<b>0.0015±0.0001</b>	1.0±0.2	<b>0.0010±0.0001</b>	4.8±0.4	<b>0.0006±0.0001</b>	78.0±9.4

Experiments are repeated five times. Testing RMSE and CPU time are in Table 9. We can see that GDPAN and TCNR achieves similar testing RMSE, and are much lower than both convex regularization (ADMM, FaLRTC, PA-APG, FFW and TNN) and factorization approach (RP, TMac, CP-OPT, TMac-TT). This again verifies that nonconvex regularization offers better empirical performance than the other approaches.

Convergence of testing RMSE vs CPU time is in Figure 4. It shows that FFW and RP are very fast but their testing RMSEs are much higher than that of TCNR. TCNR solves the same optimization problem as GDPAN, thus they have same testing RMSE. However, by utilizing the “sparse plus low-rank” structure and acceleration, TCNR is much more efficient than GDPAN, and is comparable with FFW and RP.

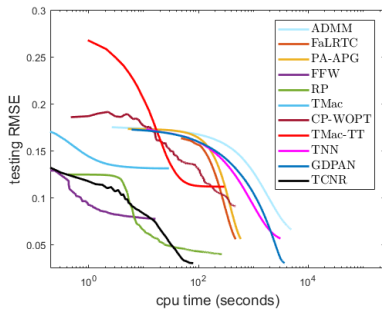
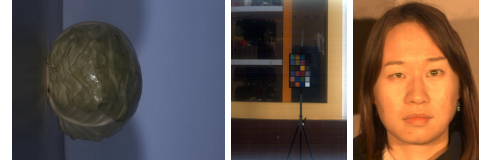


Figure 4: Testing RMSE v.s CPU time (seconds) various algorithms on the color image “Window”.

**Hyper-Spectrum Image.** Experiments are performed on hyper-spectral images (see Table 11 and Figure 5)<sup>3</sup>, the third dimension denotes the bands of images. We use the

<sup>3</sup>Female: <http://www.imageval.com/scene-database-4-faces-3-meters/> Cabbage

same setup as for the color image. ADMM, TNN, GDPAN are not compared as they are too slow; TMac-TT is also not compared as the initialization is too slow (Table 9).



(a) Cabbage. (b) Scene. (c) Female.

Figure 5: Hyperspectral images used in the experiment.

Experiments are repeated five times. Performance is shown in Table 10. Again, we can see that, as nonconvex regularizations can less penalize large singular values, TCNR can achieve much lower testing RMSE than both convex and factorization based approaches.

Testing RMSE v.s. CPU time is shown in Figure 6. The lowest RMSE is offered by TCNR, and it is much faster than all other approaches except for TMac and FFW. While TMac and FFW are very fast, their testing RMSEs are much higher than that of TCNR. Thus, TCNR is very efficient and offers good empirical performance.

**Link Prediction.** Finally, we perform experiments on the *YouTube* data set<sup>4</sup> (Lei, Wang, and Liu 2009). It contains 15,088 users, and describes five types of user interactions: contact, number of shared friends, number of shared subscriptions, number of shared subscribers, and the number of shared favorite videos. Thus, it forms a  $15088 \times 15088 \times 5$  tensor, with a total of 27,257,790 nonzero elements.

and Scene: <https://sites.google.com/site/hyperspectralcolorimaging/dataset>

<sup>4</sup><http://socialcomputing.asu.edu/datasets/YouTube>

Table 8: Algorithms used for experimental comparisons in Section 4.2.

	algorithm	model	description
convex	ADMM (Tomioka, Hayashi, and Kashima 2010)	overlapped nuclear norm	ADMM
	FaLRTC (Liu et al. 2013)		Accelerated PG algorithm for the dual problem
	PA-APG (Yu 2013)		Accelerated PA algorithm
	FFW (Guo, Yao, and Kwok 2017)	latent nuclear norm	efficient Frank-Wolfe algorithm
	TNN (Zhang and Aeron 2017)	tensor-SVD	ADMM
factorization	RP (Kasai and Mishra 2016)	Turker decomposition	Riemannian preconditioning
	TMac (Xu et al. 2013)	multiple matrices factorization	alternative minimization
	CP-WOPT (Acar et al. 2011)	CP decomposition	gradient descent
	TMac-TT (Bengua et al. 2017)	tensor-train decomposition	alternative minimization
nonconvex	GDPAN (Zhong and Kwok 2014)	nonconvex overlapped regularization	nonconvex PA algorithm
	TCNR (Algorithm 3)		proposed algorithm

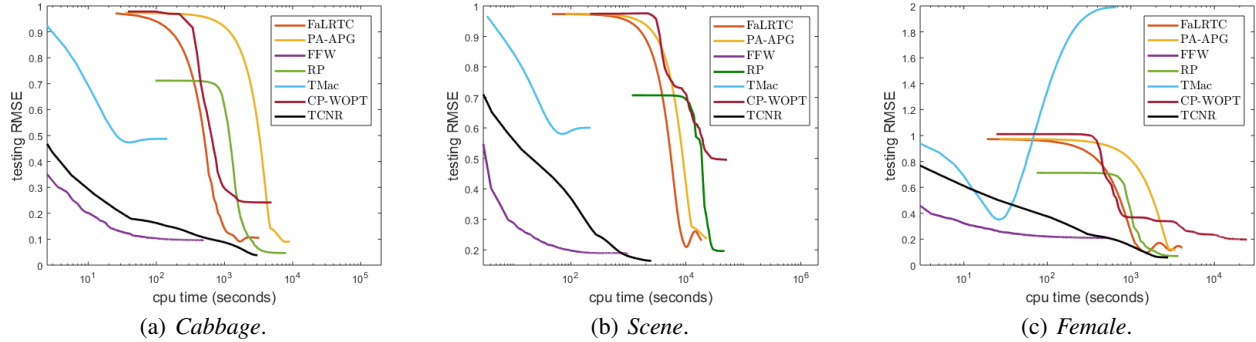


Figure 6: Testing RMSE vs CPU time (minutes) on hyperspectral images.

Table 9: Performance comparison of various algorithms on the color image *Window*. The CPU time is in seconds. The best and comparable results (according to the pairwise t-test with 95% confidence) are highlighted. Note that TMac-TT needs about 445 seconds for initialization.

	algorithm	RMSE	time (sec)
convex	ADMM	0.0661±0.0006	4890.2±46.0
	FaLRTC	0.0559±0.0014	474.9±21.5
	PA-APG	0.0561±0.0007	588.8±9.2
	FFW	0.0774±0.0006	<b>16.4±0.8</b>
	TNN	0.0567±0.0005	3108.4±90.9
factorization	RP	0.0450±0.0021	265.1±9.4
	TMac	0.1313±0.0005	28.9±2.5
	CP-OPT	0.0911±0.0122	472.8±132.5
	TMac-TT	0.1118±0.0104	294.1±101.7
nonconvex	GDPAN	<b>0.0305±0.0004</b>	3713.8±114.2
	TCNR	<b>0.0304±0.0002</b>	80.2±3.1

Following (Guo, Yao, and Kwok 2017), we formulate multi-relational link prediction as a tensor completion problem.

Here, we perform experiments on both a small *YouTube* subset, which is obtained by random selecting 1000 users (leading to 12,101 observations), and the full *Youtube* dataset. We use 50% of the observations for training, another 25% for validation and the remaining for testing.

Experiments are repeated five times. Results are in Table 12 and testing RMSE v.s. CPU time is in Figure 7. In these datasets, we can see TCNR not only achieves lower testing RMSEs but also runs much faster than other algorithms. This again demonstrates that TCNR is very

efficient and offers good empirical performance.

## 5 Conclusion

In this paper, we propose a new low-rank tensor completion model with nonconvex regularizations. While the nonconvex proximal average (PA) algorithm is the only applicable algorithm, it has large space demand and expensive iteration complexity. To address these problems, we show how proximal steps in PA algorithm can be computed efficiently and how its slow convergence can be sped up with acceleration. The convergence to critical points is of the new algorithm still guaranteed. Finally, experimental comparison of the proposed approach with various other tensor completion approaches demonstrates that the proposed algorithm is very efficient and nonconvex regularization can produce better empirical performance.

## References

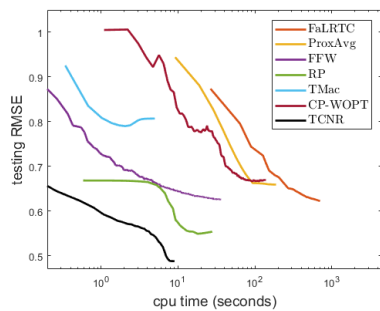
- Acar, E.; Dunlavy, D.; Kolda, T.; and Mørup, M. 2011. Scalable tensor factorizations for incomplete data. *Chemometrics and Intelligent Laboratory Systems* 106(1):41–56.
- Andersson, F.; Carlsson, M.; and Perfekt, K.-M. 2016. Operator-lipschitz estimates for the singular value functional calculus. *Proceedings of the American Mathematical Society* 144(5):1867–1875.
- Bader, B., and Kolda, T. 2007. Efficient MATLAB computations with sparse and factored tensors. *SIAM Journal on Scientific Computing* 30(1):205–231.

Table 10: Recovery performance on hyperspectral images. The RMSE is scaled by  $10^{-3}$ , CPU time is in minutes. The best and comparable results (according to the pairwise t-test with 95% confidence) are highlighted.

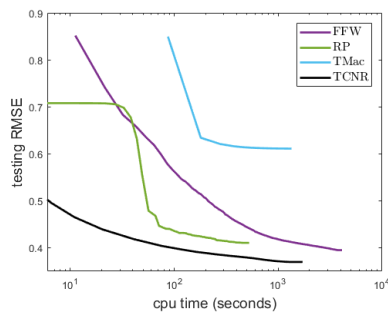
	algorithm	Cabbage		Scene		Female	
		RMSE	time (min)	RMSE	time (min)	RMSE	time (min)
convex	FaLRTC	10.50±0.12	54.0±9.2	23.08±0.24	313.3±122.7	13.33±0.04	69.0±11.6
	PA-APG	9.04±0.04	152.7±15.8	23.69±0.24	390.5±71.0	11.57±0.03	57.0±10.4
	FFW	9.62±0.04	8.3±0.1	18.89±0.08	16.5±1.5	20.96±0.06	<b>9.2±2.0</b>
factorization	RP	4.67±0.11	133.4±1.3	19.61±0.05	784.7±263.0	6.47±0.03	62.0±35.3
	TMac	48.73±0.59	<b>2.4±0.1</b>	60.06±0.08	<b>3.7±0.7</b>	198.97±0.06	11.1±3.2
	CP-OPT	24.17±4.24	81.9±41.2	49.54±3.01	876.2±172.2	19.75±1.44	409.6±70.7
nonconvex	TCNR	<b>3.79±0.12</b>	50.9±3.4	<b>16.40±0.01</b>	41.6±2.9	<b>5.93±0.14</b>	46.7±7.5

Table 11: Statistic of hyperspectral images.

	size
Cabbage	1312 × 432 × 49
Scene	1312 × 951 × 49
Female	592 × 409 × 148



(a) Small subset.



(b) Full set.

Figure 7: Testing RMSE v.s CPU time (seconds) on Youtube dataset.

Bengua, J.; Phien, H.; Tuan, H.; and Do, M. 2017. Efficient tensor completion for color image and video recovery: Low-rank tensor train. *IEEE Transactions on Image Processing* 26(5):2466–2479.

Boyd, S.; Parikh, N.; Chu, E.; Peleato, B.; and Eckstein, J. 2011. Distributed optimization and statistical learning via the alternating direction method of multipliers. *Foundations and Trends in Machine Learning* 3(1):1–122.

Candès, E., and Recht, B. 2009. Exact matrix completion via convex optimization. *Foundations of Computational Mathematics* 9(6):717–772.

Candès, E.; Wakin, M.; and Boyd, S. 2008. Enhancing sparsity by reweighted  $\ell_1$  minimization. *Journal of Fourier*

*Analysis and Applications* 14(5-6):877–905.

Chandrasekaran, V.; Recht, B.; Parrilo, P. A.; and Willsky, A. S. 2012. The convex geometry of linear inverse problems. *Foundations of Computational mathematics* 12(6):805–849.

Cheng, H.; Yu, Y.; Zhang, X.; Xing, E.; and Schuurmans, D. 2016. Scalable and sound low-rank tensor learning. In *Artificial Intelligence and Statistics*, 1114–1123.

Fan, J., and Li, R. 2001. Variable selection via nonconcave penalized likelihood and its oracle properties. *Journal of the American Statistical Association* 96(456):1348–1360.

Gandy, S.; Recht, B.; and Yamada, I. 2011. Tensor completion and low-n-rank tensor recovery via convex optimization. *Inverse Problems* 27(2):025010.

Ghadimi, S., and Lan, G. 2016. Accelerated gradient methods for nonconvex nonlinear and stochastic programming. *Mathematical Programming* 156(1-2):59–99.

Gui, H.; Han, J.; and Gu, Q. 2016. Towards faster rates and oracle property for low-rank matrix estimation. In *Proceedings of the 33rd International Conference on Machine Learning*, 2300–2309.

Guo, X.; Yao, Q.; and Kwok, J. 2017. Efficient sparse low-rank tensor completion using the Frank-Wolfe algorithm. In *Proceedings of the 21st AAAI Conference on Artificial Intelligence*, 1948–1954.

Halko, N.; Martinsson, P.-G.; and Tropp, J. 2011. Finding structure with randomness: Probabilistic algorithms for constructing approximate matrix decompositions. *SIAM Review* 53(2):217–288.

Hillar, C., and Lim, L.-H. 2013. Most tensor problems are NP-hard. *Journal of the ACM* 60(6).

Hu, Y.; Zhang, D.; Ye, J.; Li, X.; and He, X. 2013. Fast and accurate matrix completion via truncated nuclear norm regularization. *IEEE Transactions on Pattern Analysis and Machine Intelligence* 35(9):2117–2130.

Jacob, L.; Obozinski, G.; and Vert, J.-P. 2009. Group lasso with overlap and graph lasso. In *Proceedings of the 26th International Conference on Machine Learning*, 433–440.

Kasai, H., and Mishra, B. 2016. Low-rank tensor completion: a Riemannian manifold preconditioning approach. In *Proceedings of the 33rd International Conference on Machine Learning*, 1012–1021.

Kolda, T., and Bader, B. 2009. Tensor decompositions and applications. *SIAM Review* 51(3):455–500.

Table 12: Recovery performance on *Youtube* data set. CPU time is in seconds. Note that FaLRTC, PA-APG and CP-OPT are too slow, thus are not run on the full set. The best and comparable results (according to the pairwise t-test with 95% confidence) are highlighted.

	algorithm	subset		full set	
		RMSE	time (sec)	RMSE	time (sec)
convex	FaLRTC	0.622±0.060	701.7±32.0	—	—
	PA-APG	0.659±0.047	188.2±36.7	—	—
	FFW	0.626±0.054	35.9±1.9	0.395±0.001	4110.9±71.0
factorization	RP	0.554±0.026	27.8±2.3	0.410±0.001	<b>524.9±15.4</b>
	TMac	0.807±0.035	<b>5.0±2.9</b>	0.611±0.007	1343.3±224.7
	CP-OPT	0.667±0.016	132.7±15.8	—	—
nonconvex	TCNR	<b>0.488±0.017</b>	9.0±1.2	<b>0.370±0.001</b>	1717.1±77.2

Lei, T.; Wang, X.; and Liu, H. 2009. Uncovering groups via heterogeneous interaction analysis. In *IEEE International Conference on Data Mining*, 503–512.

Li, H. and Lin, Z. 2015. Accelerated proximal gradient methods for nonconvex programming. In *Advances in Neural Information Processing Systems*, 379–387.

Liu, J.; Musialski, P.; Wonka, P.; and Ye, J. 2013. Tensor completion for estimating missing values in visual data. *IEEE Transactions on Pattern Analysis and Machine Intelligence* 35(1):208–220.

Lu, C.; Tang, J.; Yan, S.; and Lin, Z. 2016. Nonconvex nonsmooth low rank minimization via iteratively reweighted nuclear norm. *IEEE Transactions on Image Processing* 25(2):829–839.

Mazumder, R.; Hastie, T.; and Tibshirani, R. 2010. Spectral regularization algorithms for learning large incomplete matrices. *Journal of Machine Learning Research* 11:2287–2322.

Mazumder, R.; Saldana, D.; and Weng, H. 2018. Matrix completion with nonconvex regularization: Spectral operators and scalable algorithms. Technical report, MIT Center for Statistics.

Mu, C.; Huang, B.; Wright, J.; and Goldfarb, D. 2014. Square deal: Lower bounds and improved relaxations for tensor recovery. In *International Conference on Machine Learning*, 73–81.

Nesterov, Y. 1983. A method for solving the convex programming problem with convergence rate  $o(1/k^2)$ . *Dokl. Akad. Nauk SSSR* 269:543–547.

Oseledets, I. 2011. Tensor-train decomposition. *SIAM Journal on Scientific Computing* 33(5):2295–2317.

Parikh, N., and Boyd, S. 2013. Proximal algorithms. *Foundations and Trends in Optimization* 1(3):123–231.

Signoretto, M.; Van de Plas, R.; De Moor, B.; and Suykens, J. 2011. Tensor versus matrix completion: a comparison with application to spectral data. *IEEE Signal Processing Letters* 18(7):403–406.

Song, Q.; Ge, H.; Caverlee, J.; and Hu, X. 2017. Tensor completion algorithms in big data analytics. Technical report, Department of Computer Science and Engineering, Texas A&M University.

Tomioka, R., and Suzuki, T. 2013. Convex tensor decomposition via structured Schatten norm regularization.

In *Advances in neural information processing systems*, 1331–1339.

Tomioka, R.; Suzuki, T.; Hayashi, K.; and Kashima, H. 2011. Statistical performance of convex tensor decomposition. In *Advances in Neural Information Processing Systems*, 972–980.

Tomioka, R.; Hayashi, K.; and Kashima, H. 2010. Estimation of low-rank tensors via convex optimization. *arXiv preprint arXiv:1010.0789*.

Xu, Y.; Hao, R.; Yin, W.; and Su, Z. 2013. Parallel matrix factorization for low-rank tensor completion. *Inverse Problems & Imaging* 9(2):601–624.

Yao, Q.; Kwok, J.; Gao, F.; Chen, W.; and Liu, T.-Y. 2017a. Efficient inexact proximal gradient algorithm for nonconvex problems. In *Proceedings of the 26th International Joint Conference on Artificial Intelligence*, 3308–3314.

Yao, Q.; Kwok, J.; Wang, T.; and Liu, T.-Y. 2017b. Large-scale low-rank matrix learning with nonconvex regularizers. *IEEE Transactions on Pattern Analysis and Machine Intelligence*.

Yu, Y.-L. and Xun, Z.; Micol, M.; and Xing, E. 2015. Minimizing nonconvex non-separable functions. In *Proceedings of the Eighteenth International Conference on Artificial Intelligence and Statistics*, 1107–1115.

Yu, Y.-L. 2013. Better approximation and faster algorithm using the proximal average. In *Advances in Neural Information Processing Systems*, 458–466.

Zhang, Z., and Aeron, S. 2017. Exact tensor completion using t-svd. *IEEE Transactions on Signal Processing* 65(6):1511–1526.

Zhang, C. 2010a. Nearly unbiased variable selection under minimax concave penalty. *Annals of Statistics* 38(2):894–942.

Zhang, T. 2010b. Analysis of multi-stage convex relaxation for sparse regularization. *Journal of Machine Learning Research* 11:1081–1107.

Zhong, W., and Kwok, J. 2014. Gradient descent with proximal average for nonconvex and composite regularization. In *Proceedings of the 28th AAAI Conference on Artificial Intelligence*, 2206–2212.